Published in final edited form as:
Faraday Discuss. 2013 ; 161: 461–589.

Interactions of Drugs and Amphiphiles with Membranes: Modulation of Lipid Bilayer Elastic Properties by Changes in Acyl Chain Unsaturation and Protonation

Michael J. Bruno[1,3,*], **Radda Rusinova**[1,*], **Nicholas J. Gleason**[2], **Roger E. Koeppe II**[2], and **Olaf S. Andersen**[1]

[1]Department of Physiology and Biophysics, Weill Cornell Medical College, New York, New York 10065, USA

[2]Department of Chemistry and Biochemistry, University of Arkansas, Fayetteville, Arkansas 72701, USA

[3]Department of Chemistry, Guilford College, Greensboro, NC 27410, USA

Abstract

Poly-unsaturated fatty acids (PUFAs) alter the function of many membrane proteins, whereas monounsatured fatty acids generally are inert. We previously showed that docosahexaenoic acid (DHA) at pH 7 decreases the bilayer stiffness, consistent with an amphiphile-induced increase in elasticity, but not with a negative change in curvature; oleic acid (OA) was inert (Bruno, Koeppe and Andersen, Proc. Natl. Acad. Sci. USA 104:9638–9643, 2007). To further explore how PUFAs and other amphiphiles may alter lipid bilayer properties, and thus membrane protein function, we examined how changes in acyl chain unsaturation, and head group charge and size, alter bilayer properties, as sensed by bilayer-spanning gramicidin A (gA) channels of different lengths. Compared to DHA, the neutral DHA-methyl ester has reduced effects on bilayer properties, and 1-palmitoyl-2-docosahexaenoyl-phosphatidylcholine (PDPC) forms bilayers that are softer than dioleoylphosphatidylcholine (DOPC). The changes in channel function are larger for the short gA channels, indicating that changes in elasticity dominate over changes in curvature. We altered the fatty acid protonation by titration: docosahexaenoic acid (DHA) is more potent at pH 9 (relative to pH 7) and is inert at pH 4; OA, which was inert at pH 7, becomes a potent modifier of bilayer properties at pH 9. At both pH 7 and 9, DHA and OA produced larger changes in the lifetimes of the short gA channels, demonstrating that they increase lipid bilayer elasticity when deprotonated —though OA promotes the formation of inverted hexagonal phases at pH 7. The positively charged oleylamine (OAm), which has a small head-group and therefore should be a negative curvature promoter, inhibited gA channel function, with similar reductions in the lifetimes of the short and long gA channels, indicating a curvature-dominated effect. Monitoring the single-channel conductance, we find that the negatively charged fatty acids increase the conductance by increasing the local negative charge around the channel, whereas the positively charged OAm has no effect. These results suggest that deprotonated fatty acids increase bilayer elasticity by reversibly adsorbing at the bilayer/solution interface.

[*]Co-first authors and authors to whom correspondence should be addressed: brunomj@guilford.edu and rar2021@med.cornell.edu. Address for editorial correspondence: Olaf S. Andersen, Department of Physiology and Biophysics, Weill Cornell Medical College, New York, New York 10065, USA, sparre@med.cornell.edu.

INTRODUCTION

Fatty acids (FAs), including the poly-unsaturated fatty acids (PUFAs), are important components of fat and membrane phospholipids, and are as such involved in body energy metabolism and the regulation of many different cell function, for recent reviews see [1–3]. PUFAs, in particular, have been implicated as important precursors for cell signaling molecules and as regulators of membrane protein function [4, 5]. Given the many different biological processes that are modulated by PUFAs, they have both beneficial and harmful effects [6, 7]. The regulation of membrane protein function occurs, at least in part, through what appears to be membrane effects, as opposed to effects mediated through direct FA-membrane protein interactions or cellular signaling processes ([8], see also Table 1 in [9]). Using the gramicidin (gA) channels as probes, we previously reported that docosahexaenoic acid (DHA), an important PUFA in fish oil, alters bilayer properties in a manner that may account for some of DHA's acute effects on ion channel function, whereas mono-unsaturated oleic acid OA was inert [9]. This pattern is similar to what has been observed for other ion channels, and membrane-active compounds like Triton X-100 can elicit similar changes in cellular excitability as DHA [8], suggesting that these changes indeed are due to altered bilayer properties as opposed to direct fatty acid-membrane protein interactions.

Our previous study [9] left open the question why OA was inert. The partition coefficient of OA into lipid bilayers is higher than that of DHA, so bilayer-incorporated OA must somehow interact differently with the lipid bilayer (membrane lipids) than DHA. It was in this context striking that OA caused little change in the single-channel channel currents, as compared to DHA [9]. The DHA-induced changes in current could arise because the adsorption of DHA imparts a negative surface charge, thereby increasing the interfacial cation concentration and thus the single-channel conductance; it also might reflect a local enrichment of DHA adjacent to the channels, which would increase the density of the more polar double bonds and thereby conceivably increase the single-channel conductance through a reduction of the electrostatic barrier for ion movement through the channel, cf. [10]. The latter mechanism could explain why OA is inert, but it is not clear that changes in the electrostatic barrier would be sufficient to account for the observed conductance changes —nor is it clear to what extent the DHA-induced changes in bilayer properties that were reported by the gA channels reflect simply the presence of poly-unsaturated acyl chain, which would be expected to alter both intrinsic curvature and bilayer elasticity, or whether the head group charge is important as well. (The poly-unsaturated acyl chains may alter also the bilayer "fluidity"; we consider this issue in the Discussion.)

We therefore explored the relative importance of acyl unsaturation and carboxylate charge fatty acids' ability to modify lipid bilayer properties—as probed using gA channels, which in this context is a generic bilayer-spanning protein. The role of acyl chain unsaturation was probed in experiments where we added poly-unsaturated acyl chains, keeping the charge invariant—by either adding the polyunsaturated acyl chain as the neutral methyl ester derivative of DHA (DHA-ME), or by incorporating it into the phospholipid *per se*, in the form of 1-palmitoyl-2-docosahexaenoyl- phosphatidylcholine (PDPC). The role of charge was probed in experiments with DHA or OA in which we varied the pH of the electrolyte solution.

The principles underlying using gA channels as probes to detect changes in bilayer properties, as sensed by a bilayer-spanning channel, are illustrated in Figure 1.

As is the case for other membrane-spanning proteins, gA channels will locally reorganize the surrounding bilayer [11, 12]. This local bilayer deformation has an associated energetic cost, the bilayer deformation energy ($\Delta G^0_{\mathrm{def}}$), that varies as a function of the hydrophobic

mismatch between the channel length (l) and the bilayer thickness (d_0), the channel radius and the bilayer material properties (thickness, intrinsic curvature, c_0, and the associated elastic compression and bending moduli). The difference between the bilayer deformation energy associated with the two monomers that will form the channel (ΔG^{M}_{def}) and with the conducting dimer (ΔG^{D}_{def}) becomes the bilayer contribution ($\Delta G^{D\rightarrow D}_{bilayer}=\Delta G^{D}_{def}-\Delta G^{M}_{def}$) to the total energetic cost of the monomer↔dimer transition, and the equilibrium distribution between the non-conducting monomers (M) and conducting dimers (D) will be given by:

$$\frac{[D]}{[M]}=\exp\left\{-\frac{\Delta G^{M\rightarrow D}_{protein}+\Delta G^{M\rightarrow D}_{bilayer}}{k_B T}\right\}, \quad (1)$$

where $\Delta G^{M\rightarrow D}_{protein}$ is the "intrinsic" energetic cost of channel formation (e.g., due to formation of the interface between the two subunits, which is stabilized by six hydrogen bonds), and k_B and T are Boltzmann's constant and temperature in Kelvin

The bilayer deformation energy (ΔG_{def}) associated with a local bilayer thinning can be expressed as :

$$\Delta G^{0}_{def}=H_B\cdot(l-d_0)^2+H_X\cdot(l-d_0)\cdot c_0+H_C\cdot c_0^2 \quad (2)$$

where H_B, H_X and H_C are elastic coefficients that are functions of the bilayer thickness, elastic moduli and channel radius (and include contributions from the energetic cost of redistributing the different components in a multi-component membrane, including the redistribution of the decane in our planar bilayer experiments), and c_0 the intrinsic monolayer curvature. Eq. 2 can be derived from the theory of elastic bilayer deformations [13]; a more general derivation, which is not subject to the assumptions used in the theory of elastic bilayer deformation, is obtained from a series expansion of $\Delta G^{0}_{def}(l-d_0, c_0)$ in ($l-d_0$) and c_0 [14].

The bilayer responds to the deformation by imposing a disjoining force (F_{dis}) on the channel [12, 15]

$$F_{dis}=-\frac{\partial \Delta G^{M\rightarrow D}_{def}}{\partial(l-d_0)}=2\cdot H_B\cdot(d_0-l_0)-H_X\cdot c_0. \quad (3)$$

Changes in F_{dis}—due, for example, to the adsorption of FAs at the bilayer/solution interface, which for thermodynamic reasons will tend to increase bilayer elasticity [16, 17]—will be observable as changes in τ. Moreover, because the hydrophobic mismatch-dependent and curvature-dependent contributions to F_{dis} are additive (Eq. 3), the gA channels not only become probes of changes in bilayer properties, it becomes possible to examine the relative importance of changes in curvature (c_0) and elasticity (the H coefficients) by doing experiments with gA channels of different lengths (Fig 1B).

MATERIALS AND METHODS

Materials

The naturally occurring mixture of gramicidins from *B brevis* (gD, for R. Dubos who discovered gramicidin [18]), which is ~80% [Val[1]]gA [19], was from Sigma (St. Louis, MO). The gA analogues gA(13) (formyl-L-Ala-D-Leu-L-Ala-D-Val-L-Val-D-Val-L-Trp-D-Leu-L-Trp-D-Leu-L-Trp-D-Leu-L-Trp-ethanolamine) and AgA^{-}(15) (formyl-D-Ala-Gly-D-Ala-L-Leu-D-

Ala-L-Val-D-Val-L-Val-D-Trp-L-Leu-D-Trp-L-Leu-D-Trp-L-Leu-D-Trp-ethanolamine) were synthesized and purified as described previously [20]. (The two analogues form channels that have opposite helix sense: gA(13) forms right-handed channels, AgA^{-}(15) forms left-handed channels.) Stock solutions (~10^{-6} M) were stored in methanol at −40 °C; they were diluted to 10^{-8} M to 10^{-9} M in absolute ethanol. Dioleoylphosphatidylcholine (DOPC), 1-palmitoyl-2-docosahexaenoyl-phosphatidylcholine (PDPC) and 1,2-dierucoyl-phosphatidylcholine ($DC_{22:1}PC$) from Avanti Polar Lipids (Alabaster, AL) were used as provided and stored in chloroform at −40 °C until needed. Docosahexaenoic acid (DHA, ≥98% pure), docosahexaenoic acid methyl ester (DHA-ME, ≥98% pure) and oleic acid (OA, ~99% pure) were from Sigma; oleylamine (OAm, 80 – 90% C_{18} content) was from Acros Organics (Geel, Belgium); they were used without further purification. *n*-decane, 99.9% pure, was from Chemsampco (Trenton, NJ), 8-aminonaphthalene-1,3,6-trisulfonate, disodium salt (ANTS) was from Invitrogen (Eugene, OR). Stock solutions of DHA, DHA-ME, OA and OAm (0.5 to 5 mM plus an equimolar amount of NaOH in the case of DHA and OA) were made in absolute ethanol, stabilized with 25 μM butylated hydroxytoluene (BHT) and stored under argon. They were stable against oxidation for two to three weeks and used within two weeks. Water was deionized Millipore Corp. Milli-Q water (Bedford, MA).

Bilayer formation and single-channel measurements

Single-channel measurements were done as described previously [20] using 20 mg/mL solutions of DOPC or PDPC in *n*-decane across a ~1.6 mm diameter hole in a 0.1 mm thick Teflon partition separating two compartments filled with 1 M NaCl and 10 mM HEPES (Sigma), and buffered to pH 4.0 (with 10 mM glycyl-glycine), 7.0 (with 10 mM HEPES) or pH 9.0 (with 10 mM Na_2HPO_4). The current signal was recorded with an AxoPatch 1C patch clamp (Axon Instruments, Foster City, CA), filtered at 2000 Hz, digitized at 20 kHz and digitally filtered to between 100 and 500 Hz. Single-channel current transitions were detected as described previously [21].

The gA analogues were added to both sides of the bilayer. To examine how changes in bilayer composition alter lipid bilayer properties, we used pairs of analogues having different sequence lengths, to vary the channel-bilayer hydrophobic mismatch, and opposite helical sense to prevent heterodimerization. After recording the channel activity in the absence of the bilayer modifier, DHA, DHA-ME, OA or OAm were added to both sides of the bilayer; the solutions were stirred for five min after addition and equilibrated for an additional 10 min. (The final [BHT] was < 0.1 μM; 0.5 μM BHT has no effect on channel function, results not shown.)

Single-channel current transitions were detected as described previously [21] using software written in VisualBasic. The current transitions for each channel type appear as a single peak in current transition amplitude histograms. For each channel type, lifetime histograms were constructed for channels with current transitions falling within the characteristic peak in the amplitude histogram (e.g. Figure 2). The average channel lifetimes, **τ**, were determined by fitting a single exponential distribution:

$$N(t)=N(0)\cdot\exp\{-t/\tau\}, \quad (4)$$

where $N(t)$ is the number of channels with lifetimes longer than time t, to the lifetime distributions. The reported results are averages from at least 3 independent experiments, each with 300 to 1000 channel events.

Fluorescence quench experiments

Large unilamellar vesicles (LUVs), loaded with the membrane-impermeable water-soluble fluorophore ANTS, were made of $DC_{22:1}PC$ using a four-step process of sonication, freeze-thawing, extrusion and elution following [22, 22]. The LUVs were doped with gD and incubated for 24 h at 12.5 °C before incubating the vesicles for 10 min at 25 °C in the absence or presence of either DHA or OA at the desired concentration and pH to measure the FA-induced changes in the fluorescence quench rate. The ANTS fluorescence ANTS is quenched by Tl^+, which crosses the bilayer slowly, whereas the conducting gramicidin channels are very Tl^+ permeable, meaning that the Tl^+ influx rate (the fluorescence quench rate) becomes a measure of the number of bilayer-spanning, conducting gramicidin channels in the LUV membranes. To measure the fluorescence quench rate, the ANTS-loaded LUVs were mixed with the Tl^+ quencher using a stopped-flow spectrofluorometer (Applied Photophysics, SX.20) and the fluorescence quench rate was determined by fitting a stretched exponential

$$F(t)=F(\infty)+(F(0)-F(\infty))\cdot\exp\left\{-(t/\tau_0)^{\beta}\right\}, \quad (5)$$

where $F(t)$ is fluorescence intensity at time t, β a measure of sample dispersity ($0<\beta\leq 1$), and τ_0 a parameter with units of time [23], and evaluating the time-dependent quench rate $k(t)$

$$k(t)=(\beta/\tau_0)\cdot(t/\tau_0)^{(\beta-1)} \quad (6)$$

at 2 ms. The reported results are averages from at least 3 independent experiments.

^{31}P Nuclear magnetic resonance sample preparation

Phospholipid membranes with or without OA were prepared using previously described procedure [24]. A lipid film consisting of 33 μmole of DOPC:DOPE (1:3) with or without 1 mole percent OA was prepared from a stock solution in $CHCl_3$ after removal of solvent on a rotavapor and further drying under vacuum. The lipid was hydrated for 1 h with 0.5 mL of 0.1 M buffer (titrated to the desired pH), vortexed until the lipid film was fully suspended, and centrifuged at 14,600 g for 120 min at 4 °C. The supernatant was removed, the pellet flushed with N_2, the tube was closed and the ^{31}P NMR spectrum was recorded as described [24].

Surface potential measurements

The surface potential of lipid monolayers spread at the air/water interface was measured using the ionizing electrode technique [25]. The lipid phase was 5 μL of a 20 mg/ml DOPC solution in hexadecane and the subphase was 250 mL 1 M NaCl, 1 mM MOPS, 1 mM glycyl-glycine, 1 mM sodium citrate, pH 4.0. The subphase electrode was a saturated KCl calomel electrode and the ionizing electrode was made from the polonium component of a Staticmaster brush (Model 1C200, Nuclear Products Co., El Monte, CA) soldered to a BNC cable and held ~0.25 cm from the interface. The potential was measured using a high-resistance electrometer (Keithley, Model 616).

The surface potential was measured before and after the monolayer was spread across the surface. The surface was cleaned by repeated suction of the surface to remove impurities. Before spreading the monolayer, a stable potential between +250 and +300 mV was considered to indicate a clean surface. 3 μM FA then was added to the subphase under constant stirring. The change in potential was recorded after 15 min. The pH of the subphase then was increased from pH 4 to pH 10 by incremental additions of 25 μL 1 N NaOH.

LogP

LogP was estimated using the ACD/Labs LogP algorithm at http://www.chemspider.com.

RESULTS

Changing Acyl Chain Unsaturation

To examine the relative importance of acyl chain unsaturation and charge on lipid bilayer properties, as sensed by bilayer-spanning channels (membrane proteins), we first examined the effects of the uncharged DHA-ME on gA(13) and AgA^{-}(15) channels in DOPC/*n*-decane bilayers. Like DHA [9], DHA-ME increases channel appearance rates in DOPC bilayers, as seen in the current traces in Figure 2A. Unlike DHA, DHA-ME does not increase the single-channel current transition amplitudes (Figure 2B), suggesting that it is the charge on the carboxylate that is responsible for the DHA-induced current changes. Yet DHA-ME increases the single-channel lifetimes in a dose-dependent manner (Figure 3), though to a lesser extent than DHA—and, as was found for DHA, the relative changes in τ of the shorter gA(13) channels, τ_{13}, were larger than those of the longer AgA^{-}(15) channels, τ_{15} (Figure 3), indicating that DHA-ME increases bilayer elasticity, cf. [9, 14, 26].

This conclusion was examined further in experiments with PDPC bilayers, which has a palmitoyl chain at the *sn*-1 position and a DHA at the *sn*-2 position. DOPC and PDPC have similar phosphate peak-to-peak differences (~35 Å) [27, 28], meaning that it is possible to compare gA channel function in the two membranes without introducing significant changes in thickness (though the present experiments were done in *n*-decane containing bilayers).

The single-channel current transition amplitudes of gA(13) and AgA^{-}(15) channels are similar in DOPC and PDPC bilayers (Figure 4A), whereas the lifetimes of the gA(13) and AgA^{-}(15) channels in PDPC membranes are three- and two-fold, respectively, longer than in DOPC membranes (Figure 4B), see also Table 1. Going from DOPC to PDPC, the bilayer-dependent changes in channel function are larger for the channel with the greater hydrophobic mismatch. It is not possible to interpret directly the changes in channel appearance rates between DOPC and PDPC membranes, but we needed to add five-fold less of either gA analogue to the PDPC/*n*-decane bilayers to achieve channel appearance rates comparable to those in the DOPC/*n*-decane bilayers—indicating that the dimerization constants are about 50-fold higher in the PDPC membranes, as compared to the DOPC membranes.

These results suggests that the single-channel current changes observed upon addition of DHA [9] primarily are due to the adsorption of the negatively charged DHA at the bilayer/solution interface, which produces a negative surface potential, rather than to changes in bilayer dielectric constant, which would lower the barrier for ion movement through the channel [10]. (Changes in the dielectric constant of the bilayer core do cause modest increases in single-channel conductances [29]. The similar conductances in DOPC and PDPC bilayers may suggest the dual effect of replacing two mono-unsaturated acyl chains by a saturated and a poly-unsaturated.) These results further suggest that the increases in single-channel lifetimes and bilayer elasticity are due, at least in part, to the poly-unsaturated docosahexaenoyl chain—though the lifetime changes produced by DHA-ME are less than those produced by DHA (the partition coefficient for DHA-ME, LogP 8.4, is likely to be higher than that of DHA, LogP 6.8), meaning that we cannot rule out a role for the carboxyl group charge.

Changing head group charge

To explore the possible role of charge on the DHA-induced changes in bilayer properties (as sensed by gA channels), we examined whether the effects of DHA vary as a function of pH. The pK of bilayer-adsorbed fatty acids adsorbed is about 2.0 – 2.5 pH units higher than their bulk pH of 4.5 – 5.0 [30–32]. We therefore examined the effect of DHA at pH 4, where DHA should be fully protonated, and pH to 9, where DHA should be fully deprotonated. At pH 4, DHA is as inert as OA is at pH 7—it increases neither the gA single-channel current transition amplitudes, appearance rates *nor* lifetimes (Figure 5).

At pH 9, DHA is a much more potent modifier of gA channel function than at pH 7—indeed, it was difficult to obtain recordings at DHA concentrations higher than 3 μM because of poor bilayer stability, high channel appearance frequencies and very long lifetimes. The DHA-induced changes in i and τ were several-fold larger than at pH 7, demonstrating that the charge on the carboxylate is important for the ability of DHA to increase both i and τ and, perhaps, for its ability to modulate other membrane proteins.

Does this mean that OA could modify gA channel function (lipid bilayer properties) if it were more fully deprotonated? (OA has little effect on i at pH 7, suggesting that it is more protonated than DHA when adsorbed at the bilayer/solution interface [9].) We therefore examined whether OA alters gA channel function at pH 9 (Figure 6).

Compared to pH 7, where OA is inert (Fig. 6A), OA produced robust changes in single-channel currents and lifetimes at pH 9 (Figure 6B and 6C). The τ-[OA] dose-response curve (Figure 7) shows that OA at pH 9 is a more potent bilayer-modifier than DHA at pH 7 (Figure 3).

Fatty acids are negative curvature promoters [33]. But, whatever the pH, neither DHA nor OA alter gA single-channel properties in a manner that is consistent with a primary role of negative changes in curvature in the regulation of gA channel function—and the OA-induced changes in gA channel function do not results from changes in channel structure, as CD spectroscopy on [Val^1]gA incorporated into DOPC vesicles (following [20]) show that gA retains its characteristic helical structure at pH 7 and 9 in both the absence and presence of OA (H. Gu and R. E. Koeppe II, unpublished results).

Negative changes in curvature would be expected to decrease channel appearance rates and lifetimes [12, 34], contrary to what we observed. To explore this question further, we examined the effect of oleylamine (OAm) on gA channel function. The volume of the amine group in OAm, ~13 Å^3 [35], is less than that of the carboxyl group in OA, ~31 Å^3 [35] and OAm, like OA, would be expected to promote a negative curvature. Indeed, OAm promotes membrane fusion [36], which often is considered to be characteristic of molecules having negative intrinsic curvature [37], and forms inverse phases [38]. The amine group should be fully protonated at both pH 7 and 9 [31], meaning that adsorption of OAm would be expected to decrease the single-channel currents.

Figure 8 shows the dose-response curve for OAm on gA(13) and AgA$^-$(15) single-channel current transition amplitudes and lifetimes.

Rather than increase i and τ, OAm decreased both i and τ. The changes in τ are consistent with both negative changes in curvature and decreases in elasticity. Unlike OA (at pH 9) and DHA (at pH 7 and 9), however, the OAm-induced changes in τ are similar for the shorter gA(13) and the longer AgA$^-$(15) channels—and identical at pH 9 (Figure 8B), which following Eq. 3 suggests that the decreases in τ (increases in F_{dis}) result primarily from changes in curvature (c_0), not from changes in elasticity (the H coefficients). The modest

changes in *i* further suggests that there is little enrichment of OAm in the vicinity of the channels, cf. [9].

Fluorescence quenching experiments in phospholipid vesicles

For technical reasons, our planar lipid bilayer experiments are done on membranes formed using DOPC/*n*-decane suspensions. To explore whether similar results are obtained in hydrocarbon-free membranes, we also explored the bilayer-modifying effects of DHA and OA using a gA-based fluorescence-quench assay [22, 39], which monitors the rate of quenching of the fluorescent reporter ANTS by Tl^+ that enters the vesicle though gA channels in the vesicle membrane. Changes in the rate of fluorescence quenching thus becomes a measure of the number of bilayer-spanning gA channels, which will vary with changes in gramicidin monomer↔dimer equilibrium—with changes in lipid bilayer properties, as sensed by a bilayer-spanning channel. The results show that both OA and DHA are more potent bilayer modifiers at pH 9 than at 7—and that DHA inhibits channel function at pH 4, whereas OA is an inhibitor of gA channel function at both pH 7 and pH 4 (Figure 9).

These results show that the key finding in the planar bilayer experiments, that OA and DHA at pH 9 shift the equilibrium distribution between non-conducting monomers and conducting dimers toward the conducting dimers (channels) is not due to the hydrocarbon used in the electrophysiological experiments.

Effects of fatty acids on the phospholipid phase preference

To further explore the effects of OA on the intrinsic lipid curvature, we examined how OA altered the lamellar↔inverse hexagonal (H_{II}) phase preference at pH 4 and 7 (it was not possible to get results at pH 9 due to lipid hydrolysis) using ^{31}P NMR (Figure 10).

The 40 °C (and 0% OA) ^{31}P NMR spectrum is typical of the lamellar phase. As the temperature is raised, the left-most peak in the spectra (Fig 10) is characteristic for the presence of an H_{II} phase, and the central peak is characteristic of an isotropic phase. In the presence of 1% OA, the new peaks appear at lower temperatures than in the absence of OA. Table 2 summarizes our results.

These changes in the propensity to form non-bilayer phases is observed at just 1 mole percent OA, demonstrating that lipid bilayers respond to even minor amounts of amphiphile, consistent with the X-ray and NMR studies of Keller et al. [40], the mechanical studies of [41] and our electrophysiological studies [9, 14, 42]. Interestingly, the population of the isotropic phase appears to be less when OA is present.

Titrating bilayer-adsorbed fatty acids

If the changes in single-channel currents result from the charge on the FA carboxyl, which causes a negative bilayer surface charge, and the changes in single-channel lifetime also are governed by the protonation state of the FA, why does OA have so little effect on *i* and τ at pH 7, whereas DHA increases both [9]? To ascertain whether the pK_a of bilayer-adsorbed OA could be higher than that of bilayer-adsorbed DHA, we measured the changes in surface potential of DOPC monolayers in the presence of either 3 μM OA or DHA as function of pH (Figure 11).

The midpoints of the titration curves, which do not correspond to the pK_as of FAs adsorbed at the bilayer/solution interface (cf. McLaughlin and Harary [43]), are 7.5 ± 0.12 and 7.1 ± 0.05 for OA and DHA, respectively (mean ± S.D.). DHA is likely to be more deprotonated than OA at pH 7. Given the surprisingly large changes in potential, which reflect not only

changes in FA protonation but also in the mole percent of FA in the monolayer, we did not pursue this further.

DISCUSSION

There is a long history of membrane effects of drugs and other amphiphiles, dating back at least to Meyer and Overton in the early 1900s (reviewed in [44]); for recent compilations of small-molecule effects on diverse membrane proteins see [9, 14, 42, 45–48]). Amphiphiles can, in principle, alter membrane protein function by many different mechanisms, ranging from binding to specific sites to altering the material properties of the host bilayer (Figure 12). In this study we examined a rather simple case of how amphiphiles alter lipid bilayer properties, as sensed by bilayer-spanning channels, as a prototypical example of membrane protein modulation by small molecules.

The simplicity arises because the structure of the gA channel effectively excludes specific binding. The phospholipid ester and phosphate oxygens may form (transient) hydrogen bonds with the indole NHs [49], but there are no stereospecific interactions between gA channels and their host bilayer [50]. We therefore discuss our results in the context of mechanisms 4 and 5 in Figure 12.

Amphiphiles as bilayer modifiers

An amphiphile's polar surface area to non-polar volume ratio usually will differ from that of the bilayer-forming lipids, meaning that the profile of intermolecular interactions along the bilayer normal (and the acyl chain dynamics) will be perturbed when amphiphiles adsorb at the bilayer/solution interface—leading to changes in bilayer properties such as: thickness, intrinsic curvature, the associated elastic compression and bending moduli, surface charge and interfacial dipole potential, and fluidity. Numerous studies show that small amphiphiles alter the bilayer bending [41, 51, 52] and compression [16, 17, 53] moduli. These changes in bilayer elasticity occurs at amphiphile mole fractions in the membrane that may be as low as 0.001 [41]. The physical basis for the amphiphile-induced decrease in bilayer elastic moduli is that the amphiphile adsorption into the bilayers varies as a function of the stress that is imposed on the bilayer [16], which increases the degrees available for the bilayer to pack around the channel and thus gives rise to a thermodynamic softening of the bilayer [17]. In the case of the area-compression modulus, the apparent elasticity modulus (K_{ap}) in the limit of zero tension can be expressed as [17]:

$$\frac{1}{K_{ap}} = \frac{1-n}{K_A} + n \cdot \left\{ \frac{1}{K_a} + \frac{a}{2 \cdot k_B T} \right\}, \quad (7)$$

where K_A denotes the area-compression of the unmodified bilayer, n the amphiphile mole fraction in the membrane, K_a the apparent area compression modulus of the amphiphile, and a the cross sectional area of the amphiphile (which for simplicity is set equal to that of the membrane-forming lipid). A key assumption in the derivation of Eq. 7 is that the chemical potential of the amphiphile in the aqueous phase is constant, which should be valid for experiments with isolated bilayers and lipid vesicles where the volume-fraction of the lipid phase is 10^{-3} or less.

Because the changes in bilayer properties result (at least in part, see below) from the altered profile of intermolecular interactions, one should expect that a change in any one bilayer property (e.g., curvature) is associated with changes also in other properties (e.g., thickness or elastic moduli—and acyl chain dynamics or "fluidity", as well as changes in interfacial dipole potential). It thus becomes difficult to identify the key features of an amphiphile that *cause* (as opposed to correlate with) the observed changes in bilayer properties and protein

function. In the case of fatty acids, the contributions from acyl chain flexibility, charge and head-group size cannot be easily separated—and the lateral interactions between the phospholipid acyl chains and hydrophobic part of the amphiphile may, in principle, decrease or increase the elastic moduli independent of the thermodynamic softening (Eq. 7) [54].

Before proceeding, we note that a causal role of bilayer fluidity can be excluded because the FAs alter the *equilibrium* distribution between non-conducting monomers and conducting dimers by *increasing* the rate constant for channel formation and *decreasing* the rate constant for dissociation (cf. Figs. 6 and 9 and [9]), see also Lee [55]. (The lateral diffusion coefficient of bilayer-incorporated peptides varies little with changes in hydrophobic mismatch [56], and should have little effect on the relative changes in the single-channel lifetimes of channels of different length.)

Because many amphiphiles are dipolar, they also may alter the interfacial dipole potential [57], which in its own right may alter membrane protein function. It has been proposed that gA single-channel lifetimes are directly modulated by changes in the interfacial dipole potential due to the adsorption of amphiphiles [58]. The relative importance of the changes in dipole potential and the thermodynamic softening (Eq. 7) is difficult to determine, however, because reversibly adsorning amphiphiles that alter the interfacial dipole potential, such as phloretin [57] also will soften the bilayer (reduce K_{ap}, Eq. 7). Indeed, amphiphiles such as Triton X-100 and lysophosphatidylcholine, which are known to shift the gramicidin monomer↔dimer equilibrium toward the conducting dimers [59, 60], similar to phloretin [61], produce positive changes in the interfacial dipole potential as opposed to the negative changes observed with phloretin (D. B. Sawyer and O. S. Andersen, unpublished results)

Acyl unsaturation and gramicidin channel function

The experiments with neutral DHA-ME and zwitterionic PDPC show that introducing the poly-unsaturated DHA chain, whether by the adsorption of DHA-ME or by incorporation into the bilayer-forming phospholipid, increases single-channel lifetimes—with the larger changes in **τ** being observed for the short gA(13), as compared to the long AgA^-(15) channels (Figs. 2 – 4, Table 1). The changes in channel function thus vary with hydrophobic mismatch, meaning that DHA reduces the $2 \cdot H_B \cdot (d_0 - l_0)$ contribution to F_{dis} (cf. Eq. 3). The amphiphile-induced changes in H_B can be estimated as [12, 14]

$$H_B^{amph} - H_B^{cntrl} = \frac{k_B T}{2 \cdot \delta \cdot (l_{13} - l_{15})} \ln \left\{ \frac{\tau_{15}^{cntrl} \cdot \tau_{13}^{amph}}{\tau_{15}^{amph} \cdot \tau_{13}^{cntrl}} \right\}, \quad (8)$$

where the subscripts 13 and 15 denote the two channel types. δ ≈ 0.16 nm and $l_{15} - l_{13} \approx$ 0.32 nm [26, 62]. Using Eq. 8 we find that 10 μM DHA-ME (nominal concentration; the actual aqueous concentration is ~100 nM, estimated following [9], see below) decreases the elastic coefficient H_B by 2.3 ± 0.7 $k_B T$/nm^2 (6 ± 2 kJ/(mole·nm^2), a 10% decrease from the control value of 56 kJ/(mole·nm^2) [12]. The decrease may seem modest, but is sufficient to decrease the $H_B \cdot (d_0 - l_0)^2$ contribution to $\Delta G_{bilayer}^{M \to D}$ by 7.5 $k_B T$ (for l = 2.2 nm [11, 63] and d_0 = 4.0 nM [26]). Similarly one can estimate ΔH_B going from DOPC to PDPC membranes to be −2.8 ± 0.7 $k_B T$/nm^2. The increased flexibility of the poly-unsaturated DHA chain [64] increases bilayer elasticity, consistent with the finding that multiple double bonds decrease the bilayer bending modulus [65].

The changes in single-channel lifetimes are not related to changes in ion permeability because the single-channel current amplitudes in PDPC and DHA-ME membranes were similar to those in DOPC membranes (Figs. 2 – 4); see also [34]. These results further suggest that the increased conductance produced by DHA [9] is primarily due to the

negative charge on the (at least partly) deprotonated DHA, not an increase in the dielectric constant in the bilayer hydrophobic core due to the incorporation of double bonds (cf. [29]).

Carboxyl group protonation state and gramicidin channel function

The charge on the fatty acid is important also for the changes in bilayer properties because DHA at pH 7 produced greater changes in τ than DHA-ME. The relative changes in τ_{13} were again larger than those in τ_{15}, and 10 μM DHA (nominal concentration) decreases H_B by 4.2 ± 0.9 k_BT/nm^2, a 20% decrease relative to control (DOPC). The mole fractions of DHA-ME and DHA in the membrane were similar, ~0.03, meaning that DHA is more bilayer-modifying than DHA-ME. (The mole fractions were estimated from bilayer partition coefficients following [9], using the ADIFAB method [66]. The method fails for DHA-ME, which has no carboxyl group, but the neutral, more hydrophobic DHA-ME would be expected to have a higher partition coefficient than DHA. As already ~99% of the added DHA is in the membrane [9], the mole fraction of DHA-ME will be similar to that of DHA.) Per molecule in the membrane, DHA is the more potent bilayer modifier—at least at pH 7, where it is partly deprotonated. The changes in membrane properties produced by 10 μM DHA (nominal concentration) are even larger than the difference between DOPC and PDPC membranes (Table 1), even though the mole fraction of DHA chains in PDPC membranes is 0.5, some 30-fold higher than in DOPC membranes doped with 10 μM DHA.

To explore further the importance of the FA protonation state on bilayer properties, as sensed by gA channels, we explored the bilayer-modifying potency of DHA at pH 4, where it had little effect on i or τ (Fig. 5). Indeed, there was a slight decrease in τ_{15}. This surprising result motivated us to examine how DHA alters gA channel function at pH 9, where it was much more active than at pH 7. It was again possible to estimate the changes in the elastic coefficient H_B; at 10 μM DHA, ΔH_B was −2.0 ± 0.6 k_BT/nm^2 at pH 4 and −10 ± 2 k_BT/nm^2 at pH 9. As the DHA carboxyl group becomes deprotonated, DHA becomes an increasingly potent bilayer modifier. Even OA, which is inert at pH 7, becomes a potent modifier of bilayer properties at pH 9 (Figs. 6 and 7). As was the case for DHA, OA increases bilayer elasticity at high pH where the carboxyl group should be fully deprotonated; at 10 μM OA, ΔH_B was indistinguishable from 0 at pH 7 and −10 ± 1 k_BT/nm^2 at pH 9.

The single-channel experiments were done using hydrocarbon-containing planar bilayers, but similar results were obtained in hydrocarbon-free lipid vesicles (Fig. 9). Both DHA and OA increase gramicidin channel activity at pH 9, as compared with pH 7, and both DHA and OA decrease the activity at pH 4. (These experiments were done with gD, the naturally occurring mix of 15 amino acid gA analogues, and are thus concordant with the pH 4 results for DHA; Fig. 5.) The reduction in gramicidin channel activity, however, are less than those produced by long-chain alcohols [54], suggesting that the relative lack of effect may result from a combination of the thermodynamic softening (Eq. 7) and acyl chain interactions that increase acyl chain order (cf. [67]).

Fatty acids promote lipid phases with negative curvature, e.g., [33]. It is thus surprising that DHA at pH 4 and OA at pH 7 are as inert as they are—especially given the negative shift in the lamellar→H_{II} phase transition temperature at pH 7 (Fig. 10), which raises the possibility that mixed ionization states may be important because the pK_as of adsorbed FAs will be ~2 pH units higher than their bulk pK_a [31, 32, 68].

To further explore the role of curvature, we examined the effect of OAm, a putative H_{II} phase promoter. Contrary to OA, OAm decreases τ, with similar changes in τ_{13} and τ_{15} (Fig. 8 and Table 2), meaning that OAm does not alter the hydrophobic mismatch-dependent term in Eq. 3 and, by exclusion, that OAm inhibits gA channel function by inducing a negative change in curvature. At pH 9, the changes in i are less and the changes in τ are

greater than at pH 7, suggesting that OAm may be somewhat deprotonated at pH 9, which would be expected to reduce head group volume and hydration—such that the deprotonated OAm may produce more negative changes in curvature than the protonated form.

Finally, to further explore why DHA is a more effective bilayer modifier than OA at pH 7, we explored the surface titration of DHA and OA. In agreement with previous studies [30–32, 68], we find that the midpoint of the titration curves is shifted ~2.5 pH units positive compared to the bulk pK_a. (We do not, however, understand the basis for the magnitude of the potential change.) The shift in the titration curve for DHA is less than that of OA, but it seems unlikely that the small difference in the curves, per se, could account for the rather dramatic difference in channel modulation. A possible alternative mechanism, based on the unusual shape of the OA titration curve, is that the difference in titration curves reflect different intermolecular interactions, different acyl chain flexibility, of DHA and OA. The increased flexibility of the poly-unsaturated DHA chain would be expected to increase its limiting area in the monolayer (and bilayer). (The limiting areas of steric acid (18:0), OA (18:1) and linoleic acid (18:2) are 21 $Å^2$, 42 $Å^2$ and 48 $Å^2$, respectively [69]; the limiting area of DHA is likely to be larger than that of linoleic acid.) Increasing the limiting area would increase the intermolecular distances between carboxylic acid head groups, or between the head group and the phosphate of the phospholipid, meaning that mono-unsaturated OA is likely to have stronger interactions with neighboring phospholipids and other OAs, as compared to the poly-unsaturated DHA, which could produce a larger shift in pK_a. If OA can pack more tightly at lower pH (< 8), two OAs may be able to share a proton. Such a “double-chained” FA would be expected to have a higher partition coefficient, which could account for the more pronounced negative-going change in the titration curve for OA as compared to DHA.

We have no independent evidence for this proposal, but note that the existence of such non-covalently linked doublets would be consistent with titration studies on FAs at high concentrations [70, 71], where FAs form micelles at pH >9 and an oil phase at pH < 8, with a mixed bilayer and oil phase between pH 8 and 9. If such doublets exist, and partition less well into the perturbed bilayer adjacent to a gA channel, it would explain why OA at pH 7 is inert, as sensed by gA channels, even though it partitions strongly into the bilayer as judged from the changes in surface potential and its partition coefficient [9, 72]. At pH > 8, when OA is more fully deprotonated (and the oil phase disappears), these doublets would disappear and OA would be expected to behave more like DHA—which seems to be the case, as judged from the changes in gA channel function and from the titration experiments. In effect, the non-covalently linked doublet, with a small polar surface area as compared to the hydrophobic volume (cross-sectional area) would be expected to have a strong propensity to form H_{II} phases, whereas the fully protonated OA would have a weaker propensity—thus accounting for the pH-dependent changes in OA’s ability to promote the formation of H_{II} phases (Fig. 10 and Table 2). The deprotonated OA, would be expected to promote a positive curvature, meaning that it could partition more readily into the perturbed bilayer adjacent to a gA channel, thereby increasing τ by a combination of an increase in the local bilayer elasticity and a more positive curvature, and increasing i by adding a local negative surface charge.

Acknowledgments

This work was supported by NIH grants NIH grants GM021342 and ARRA Supplement GM021342-35S1 and RR015569. We thank Lawrence G. Palmer for suggesting that we explore the possible importance of the carboxylate charge, and Hong Gu for assistance with the circular dichroism experiments.

References

1. Schmitz G, Ecker J. Prog. Lipid Res. 2008; 47:147–155. [PubMed: 18198131]
2. Tvrzicka E, Kremmyda LS, Stankova B, Zak A. Biomed. Pap. 2011; 155:117–130.
3. Kremmyda LS, Tvrzicka E, Stankova B, Zak A. Biomed. Pap. 2011; 155:195–218.
4. Hulbert AJ, Turner N, Storlien LH, Else PL. Biol. Rev. Camb. Philos. Soc. 2005; 80:155–169. [PubMed: 15727042]
5. Adkins Y, Kelley DS. J. Nutr. Biochem. 2010; 21:781–792. [PubMed: 20382009]
6. McMurray DN, Bonilla DL, Chapkin RS. Chem Phys Lipids. 2011
7. Serini S, Fasano E, Piccioni E, Cittadini AR, Calviello G. Chem. Res. Toxicol. 2011; 24:2093–2105. [PubMed: 21902224]
8. Leaf A, Xiao YF. J. Membrane Biol. 2001; 184:263–271. [PubMed: 11891551]
9. Bruno MJ, Koeppe RE II, Andersen OS. Proc. Natl. Acad. Sci. USA. 2007; 104:9638–9643. [PubMed: 17535898]
10. Allen TW, Andersen OS, Roux B. Proc. Natl. Acad. Sci. USA. 2004; 101:117–122. [PubMed: 14691245]
11. Huang HW. Biophys. J. 1986; 50:1061–1070. [PubMed: 2432948]
12. Lundbæk JA, Collingwood SA, Ingólfsson HI, Kapoor R, Andersen OS. J. R. Soc. Interface. 2010; 7:373–395. [PubMed: 19940001]
13. Nielsen C, Andersen OS. Biophys. J. 2000; 79:2583–2604. [PubMed: 11053132]
14. Rusinova R, Herold KF, Sanford RL, Greathouse DV, Hemmings HC Jr, Andersen OS. J. Gen. Physiol. 2011; 138:249–270. [PubMed: 21788612]
15. Andersen OS, Koeppe RE II. Annu. Rev. Biophys. Biomol. Struct. 2007; 36:107–130. [PubMed: 17263662]
16. Evans, E.; Rawicz, W.; Hofmann, AF. Bile Acids in Gastroenterology: Basic and Clinical Advances. Hofmann, AF.; Paumgartner, G.; Stiehl, A., editors. Dordrecht: Kluwer Academic Publishers; 1995. p. 59-68.
17. Zhelev DV. Biophys. J. 1998; 75:321–330. [PubMed: 9649389]
18. Dubos RJ. J. Exp. Med. 1939; 70:1–10. [PubMed: 19870884]
19. Abo-Riziq A, Crews BO, Callahan MP, Grace L, de Vries MS. Angew. Chem. Int. Ed. Engl. 2006; 45:5166–5169. [PubMed: 16927327]
20. Greathouse DV, Koeppe RE II, Providence LL, Shobana S, Andersen OS. Meth. Enzymol. 1999; 294:525–550. [PubMed: 9916247]
21. Andersen OS. Biophys. J. 1983; 41:119–133. [PubMed: 6188500]
22. Ingólfsson HI, Andersen OS. Assay Drug Dev. Technol. 2010; 8:427–436. [PubMed: 20233091]
23. Berberan-Santos MN, Bodunov EN, Valeur B. Chem. Phys. 2005; 315:171–182.
24. van der Wel PC, Pott T, Morein S, Greathouse DV, Koeppe RE II, Killian JA. Biochemistry. 2000; 39:3124–3133. [PubMed: 10715134]
25. Gaines, GL, Jr. Insoluble Monolayers at Liquid-Gas Interfaces. New York: Interscience; 1966.
26. Lundbæk JA, Koeppe RE II, Andersen OS. Proc. Natl. Acad. Sci. USA. 2010; 107:15427–15230. [PubMed: 20713738]
27. Wiener MC, White SH. Biophys. J. 1992; 61:437–447.
28. Huber T, Rajamoorthi K, Kurze VF, Beyer K, Brown MF. J. Am. Chem. Soc. 2002; 124:298–309. [PubMed: 11782182]
29. Girshman J, Greathouse JV, Koeppe RE II, Andersen OS. Biophys. J. 1997; 73:1310–1319. [PubMed: 9284299]
30. Small DM, Cabral DJ, Cistola DP, Parks JS, Hamilton JA. Hepatology. 1984; 4:77S–79S. [PubMed: 6479889]
31. Froud RJ, East JM, Rooney EK, Lee AG. Biochemistry. 1986; 25:7535–7544. [PubMed: 2948559]
32. Peitzsch RM, McLaughlin S. Biochemistry. 1993; 32:10436–10443. [PubMed: 8399188]
33. Seddon JM. Biochim. Biophys. Acta. 1990; 1031:1–69. [PubMed: 2407291]

34. Lundbæk JA, Maer AM, Andersen OS. Biochemistry. 1997; 36:5695–5701. [PubMed: 9153409]
35. Zamyatnin AA. Annu. Rev. Biophys. Bioeng. 1984; 13:145–165. [PubMed: 6378067]
36. Bruckdorfer KR, Cramp FC, Goodall AH, Verrinder M, Lucy JA. J. Cell Sci. 1974; 15:185–199. [PubMed: 4601320]
37. Chernomordik LV, Kozlov MM. Nature Struct. Mol. Biol. 2008; 15:675–683. [PubMed: 18596814]
38. Kisner A, Heggen M, Tillman K, Mourzina Y, Offenhäusser. Mater. Res. Soc. Symp. 2010; 1206 1206-M16-29.
39. Ingólfsson HI, Sanford RL, Kapoor R, Andersen OS. J. Vis. Exp. 2010:e2131.
40. Keller SL, Gruner SM, Gawrisch K. Biochim. Biophys. Acta. 1996; 1278:241–246. [PubMed: 8593282]
41. Vitkova V, Meleard P, Pott T, Bivas I. Eur. Biophys. J. 2006; 35:281–286. [PubMed: 16211403]
42. Ingólfsson HI, Koeppe RE II, Andersen OS. Biochemistry. 2007; 46:10384–10391. [PubMed: 17705403]
43. McLaughlin S, Harary H. Biochemistry. 1976; 15:1941–1948. [PubMed: 946770]
44. Seeman P. Pharmacol. Rev. 1972; 24:583–655. [PubMed: 4565956]
45. Hwang TC, Koeppe RE II, Andersen OS. Biochemistry. 2003; 42:13646–13658. [PubMed: 14622011]
46. Lundbæk JA, Birn P, Tape SE, Toombes GE, Søgaard R, Koeppe RE II, Gruner SM, Hansen AJ, Andersen OS. Mol. Pharmacol. 2005; 68:680–689. [PubMed: 15967874]
47. Artigas P, Al'aref SJ, Hobart EA, Diaz LF, Sakaguchi M, Straw S, Andersen OS. Mol. Pharmacol. 2006; 70:2015–2026. [PubMed: 16966478]
48. Ingólfsson HI, Koeppe RE II, Andersen OS. FEBS Lett. 2011; 585:3101–3105. [PubMed: 21896274]
49. Kim T, Lee KI, Morris P, Pastor RW, Andersen OS, Im W. Biophys. J. 2012; 102:1551–1560. [PubMed: 22500755]
50. Providence LL, Andersen OS, Greathouse DV, Koeppe RE II, Bittman R. Biochemistry. 1995; 34:16404–16411. [PubMed: 8845367]
51. Duwe HP, Kaes J, Sackmann E. J. Phys. France. 1990; 51:945–962.
52. Zhou Y, Raphael RM. Biophys. J. 2005; 89:1789–1801. [PubMed: 15951377]
53. Ly HV, Longo ML. Biophys. J. 2004; 87:1013–1033. [PubMed: 15298907]
54. Ingólfsson HI, Andersen OS. Biophys. J. 2011; 101:847–855. [PubMed: 21843475]
55. Lee AG. Prog. Lipid Res. 1991; 30:323–348. [PubMed: 1816552]
56. Ramadurai S, Holt A, Schafer LV, Krasnikov VV, Rijkers DT, Marrink SJ, Killian JA, Poolman B. Biophys. J. 2010; 99:1447–1454. [PubMed: 20816056]
57. Andersen OS, Finkelstein A, Katz I, Cass A. J. Gen. Physiol. 1976; 67:749–771. [PubMed: 946975]
58. Rokitskaya TI, Antonenko YN, Kotova EA. Biophys. J. 1997; 73:850–854. [PubMed: 9251801]
59. Sawyer DB, Koeppe RE II, Andersen OS. Biochemistry. 1989; 28:6571–6583. [PubMed: 2477060]
60. Lundbæk JA, Andersen OS. J. Gen. Physiol. 1994; 104:645–673. [PubMed: 7530766]
61. Andersen, OS. Renal Function. Giebisch, GH.; Purcel, EF., editors. New York: Ed. The Josiah Macy, Jr. Foundation; 1978. p. 71-99.
62. Greisen P Jr, Lum K, Ashrafuzzaman M, Greathouse DV, Andersen OS, Lundbæk JA. Proc. Natl. Acad. Sci. USA. 2011; 108:12717–12722. [PubMed: 21768343]
63. Elliott JR, Needham D, Dilger JP, Haydon DA. Biochim. Biophys. Acta. 1983; 735:95–103. [PubMed: 6194820]
64. Feller SE, Gawrisch K, MacKerell AD Jr. J. Am. Chem. Soc. 2002; 124:318–326. [PubMed: 11782184]
65. Rawicz W, Olbrich KC, McIntosh T, Needham D, Evans E. Biophys. J. 2000; 79:328–339. [PubMed: 10866959]
66. Richieri GV, Ogata RT, Kleinfeld AM. Mol. Cell. Biochem. 1999; 192:87–94. [PubMed: 10331662]

67. Mabrey S, Sturtevant JM. Biochim. Biophys. Acta. 1977; 486:444–450. [PubMed: 856286]
68. Drummond CJ, Grieser F, Healy TW. J. Chem. Soc., Faraday Trans. I. 1989; 85:521–535.
69. Tomoaia-Cotisel M, Zsako J, Mocanu A, Lupea M, Chifu E. J. Coll. Interface Sci. 1987; 117:464–476.
70. Morigaki K, Walde P. Curr. Opin. Coll. Interf. Sci. 2007; 12:75–80.
71. Namani T, Ishikawa T, Morigaki K, Walde P. Colloids Surf. B Biointerfaces. 2007; 54:118–123. [PubMed: 16829059]
72. Anel A, Richieri GV, Kleinfeld AM. Biochemistry. 1993; 32:530–536. [PubMed: 8422363]
73. Andersen OS. J. Gen. Physiol. 2008; 131:395–397. [PubMed: 18411334]

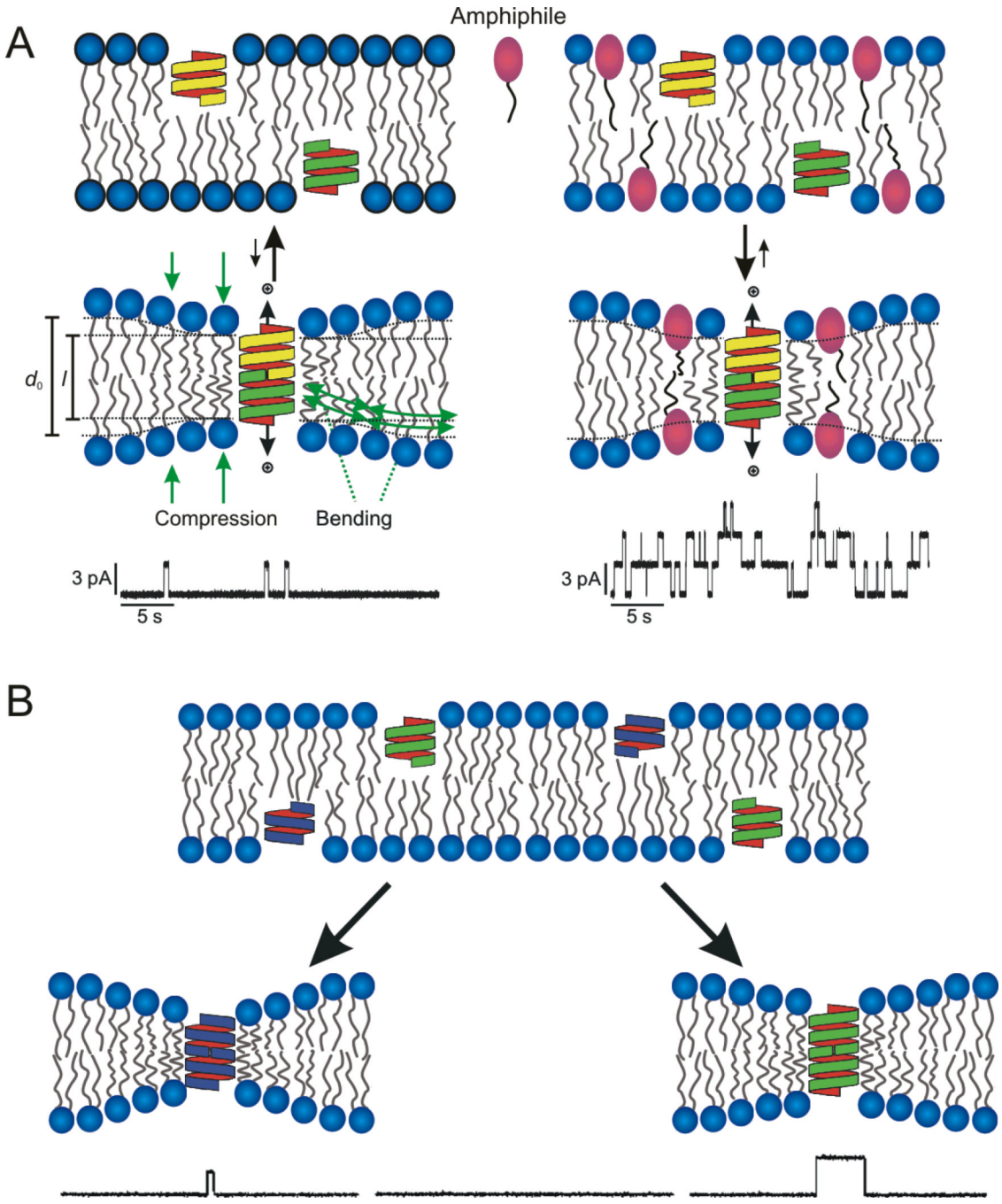

Figure 1.

Gramicidin channels as probes of changes in bilayer properties: **A**) Bilayer-spanning gA channels form by transmembrane dimerization of two $\beta^{6.3}$-helical subunits; channel formation is reported as changes in the current through the bilayer. **Left**: Because the channel length (l) is less than the unperturbed bilayer thickness (d_0), the bilayer will adapt to the hydrophobic mismatch to minimize the exposure of hydrophobic residues to water. This adaptation involves local compression of the bilayer hydrophobic core and bending of the bilayer/solution interface. Channel formation thus will incur an energetic cost, meaning that the energetic cost of channel formation—and the single-channel appearance frequency and

lifetime—varies with changes in lipid bilayer properties. **Right**: In bilayers that have been modified by the adsorption of amphiphiles at the bilayer/solution interface, the bilayer has additional degrees of freedom in terms of how it adapts to a channel-bilayer hydrophobic mismatch because the amphiphiles may redistribute between the membrane and the aqueous phases, which will tend to reduce the magnitude of the $\Delta G^{D\rightarrow D}_{bilayer}$ such that the gA monomer↔dimer equilibrium will tend to be shifted toward the conducting dimers. **B**) It is possible to use gA channels of different lengths, which can be distinguished by the magnitude of the single-channel current transitions for each channel type, to explore the relative contributions of changes in intrinsic curvature and bilayer elasticity because the hydrophobic mismatch-dependent contribution to F_{dis} (Eq. 3) will differ for channels of different length. (For practical reasons, these experiments are done with gramicidin analogues of different helix sense; this precludes the formation of heterodimers, which would complicate the analysis)

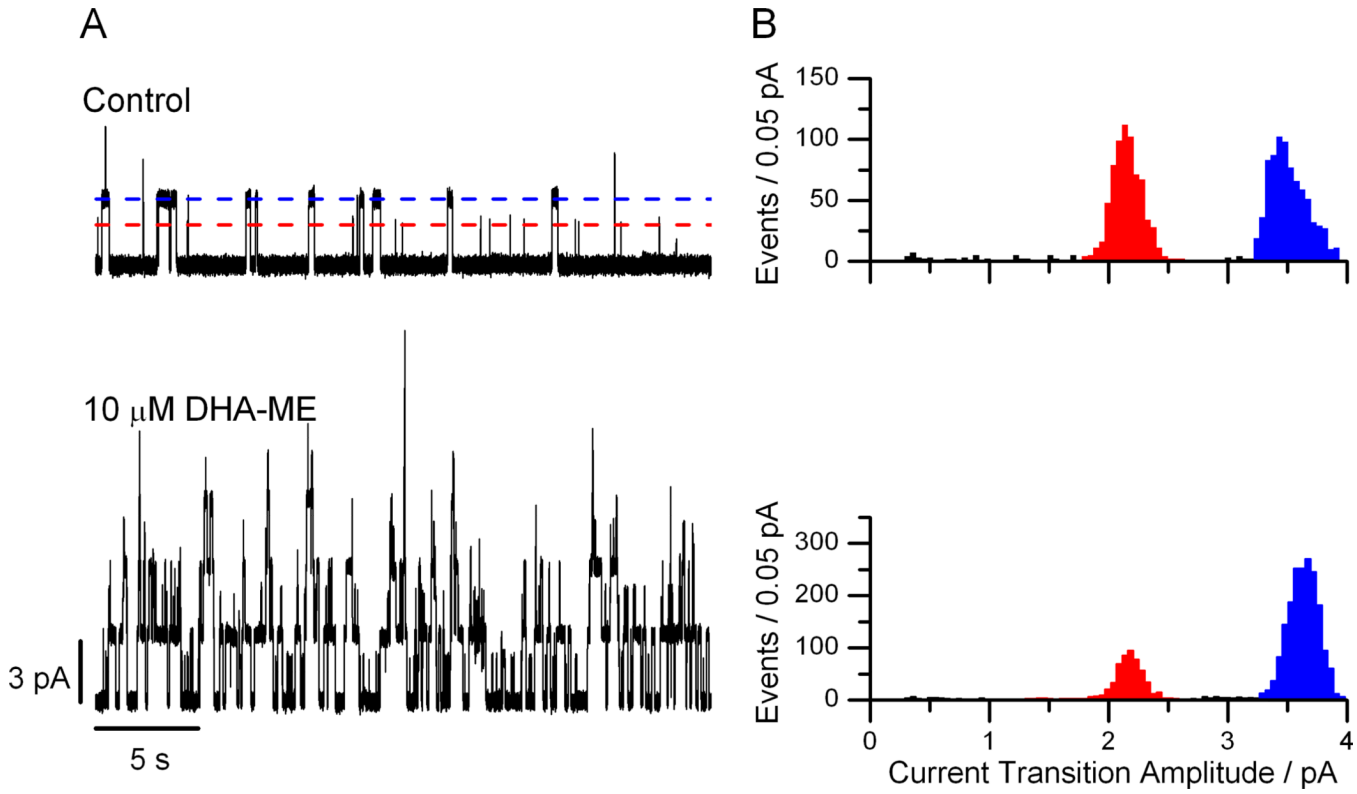

Figure 2.

DHA-methyl ester is a bilayer modifier. **A:** Current traces before and after the addition of 10 μM DHA-ME to both sides of the DOPC/*n*-decane bilayer incubated with gA(13) and $AgA^{-}(15)$. The current amplitudes of gA(13) and $AgA^{-}(15)$ channels are indicated by the red and blue lines, respectively. **B**. Current transition amplitude histograms of gA(13) (red peak) and $AgA^{-}(15)$ (blue peak) channels in the absence (top) and presence (bottom) of 10 μM DHA-ME. The current transition amplitudes for the gA(13) and $AgA^{-}(15)$ channels are (mean ± SD): 2.16 ± 0.13 pA and 3.51 ± 0.16 pA in the absence of DHA-ME and 2.17 ± 0.14 pA and 3.63 ± 0.12 pA in the presence of DHA-ME. DOPC, 1 M NaCl, 10 mM HEPES (pH 7), 200 mV.

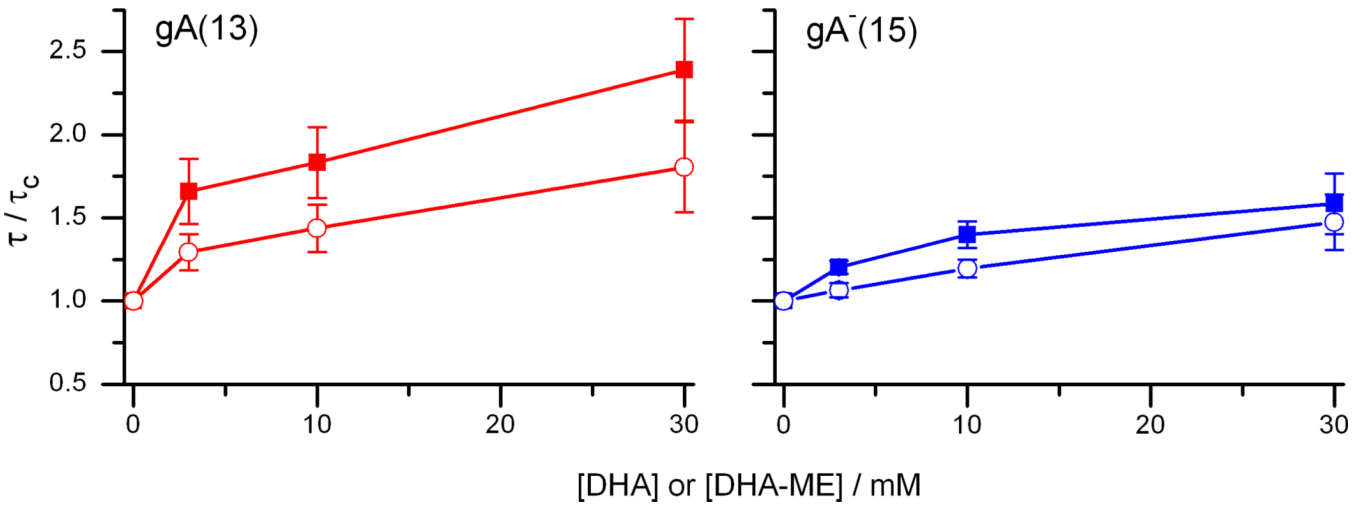

Figure 3.
DHA-methyl ester is a less potent bilayer modifier than DHA. Single-channel lifetimes of gA(13) and AgA⁻(15) channels as functions of [DHA] (closed symbols) and [DHA-ME] (open symbols). Experimental conditions as in Fig. 2.

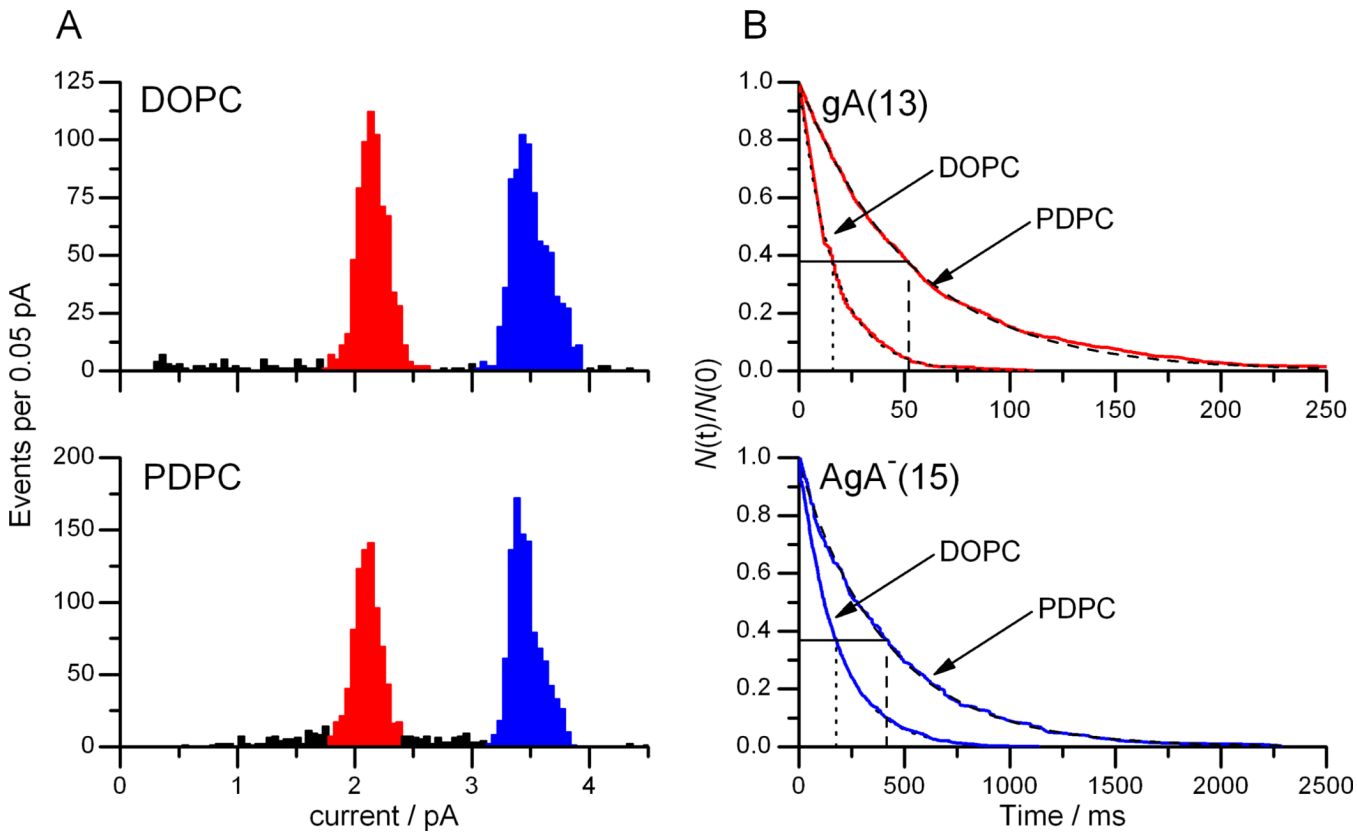

Figure 4.

Comparison of gA single-channel current transition amplitudes and lifetimes in DOPC and PDPC bilayers **A**: Current transition amplitude histograms of gA(13) (red peak) and AgA −(15) (blue peak) channels in DOPC or PDPC bilayers. **B**: Normalized single-channel survivor histograms fitted with single exponential distributions for gA(13) channels (top, τ_{DOPC} = 16 ms, τ_{PDPC} = 53 ms) and AgA−(15) channels (bottom, τ_{DOPC}=177 ms, τ_{PDPC}=414 ms). 1 M NaCl, 10 mM HEPES (pH 7), 200 mV.

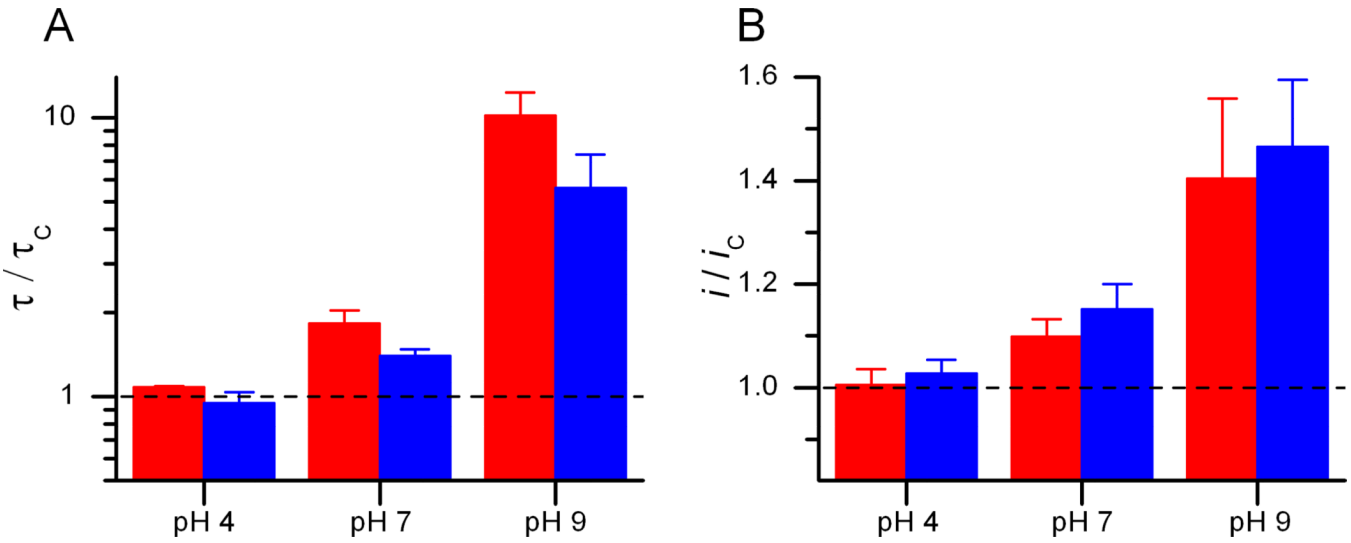

Figure 5.

The bilayer-modifying activity of DHA varies as function of pH. Changes in *i* (**A**) and **τ** (**B**) for gA(13) channels (red) and AgA−(15) channels (blue) produced by 3 μM DHA at pH 4, 7 or 9. DOPC, 1 M NaCl, 10 mM Gly-Gly (pH 4), 10 mM HEPES (pH 7) or 10 mM Na_2HPO_4 (pH 9). 200 mV.

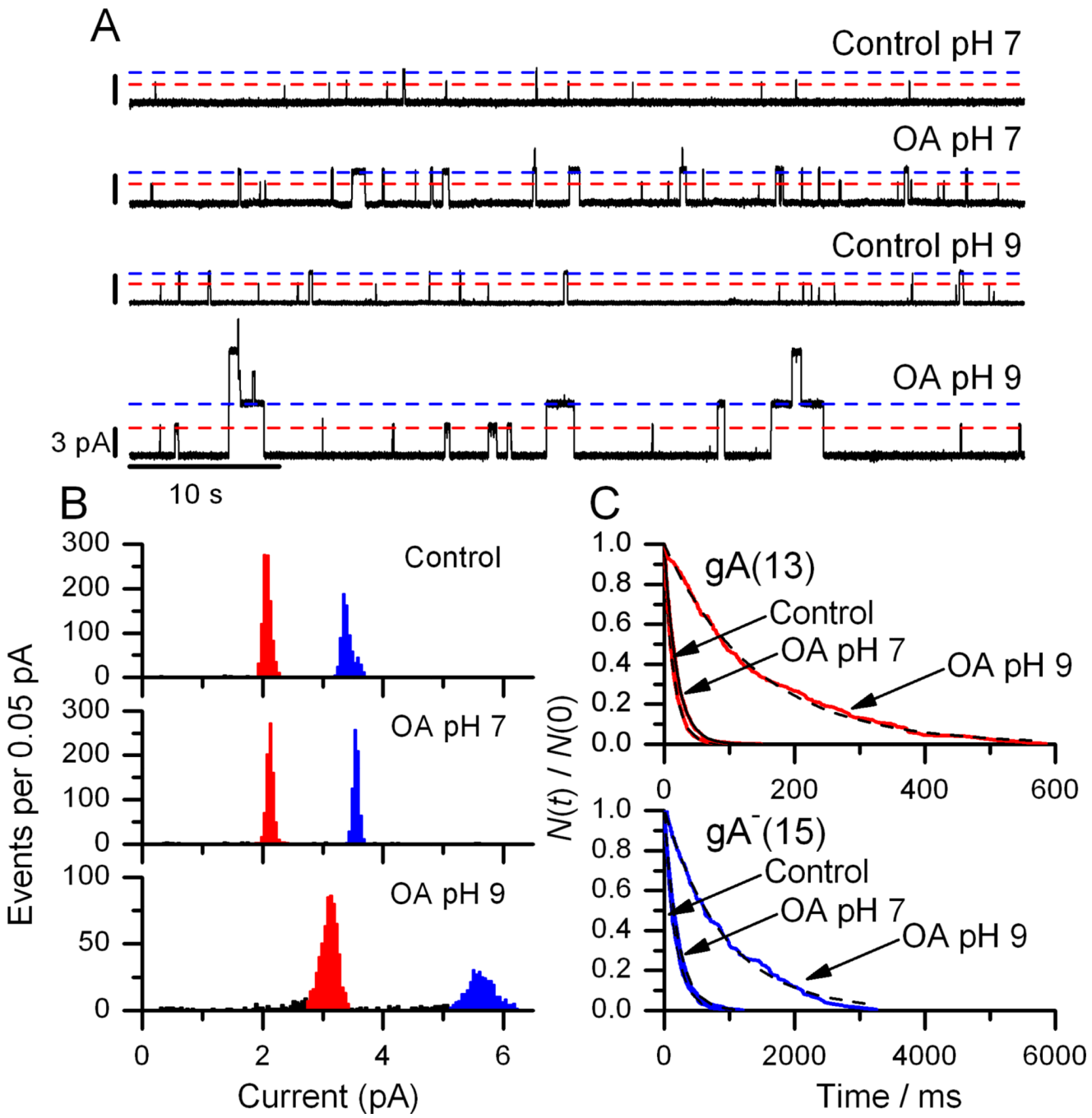

Figure 6.

OA increases gA single-channel current transition amplitudes and lifetimes at pH 9 but not at pH 7. **A:** Current traces obtained before and after the addition of 10 μM OA to both sides of DOPC/*n*-decane bilayers doped with gA(13) and AgA−(15) at pH 7 (top two traces) or pH 9 (bottom two traces). Interrupted lines denote the current levels for gA(13) (red) and AgA−(15) (blue) channels. **B**: Current transition amplitude histograms of gA(13) (red peak) and AgA−(15) (blue peak) in the absence or presence of 10 μM OA at pH 7 or 9. **C**: Single-channel survivor histograms fitted with single exponential distributions for gA(13) channels (top) ($\tau_{c,7}$ = 17 ms, $\tau_{OA,7}$ = 20 ms; $\tau_{c,9}$ = 21 ms, $\tau_{OA,9}$ = 141 ms) and AgA−(15) channels

(bottom) (τ_c=187 ms, $\tau_{OA,7}$ = 220 ms; $\tau_{c,9}$ = 217 ms, $\tau_{OA,9}$ = 917 ms). DOPC, 1 M NaCl, 10 mM HEPES (pH 7) or 10 mM Na_2HPO_4 (pH 9), 200 mV.

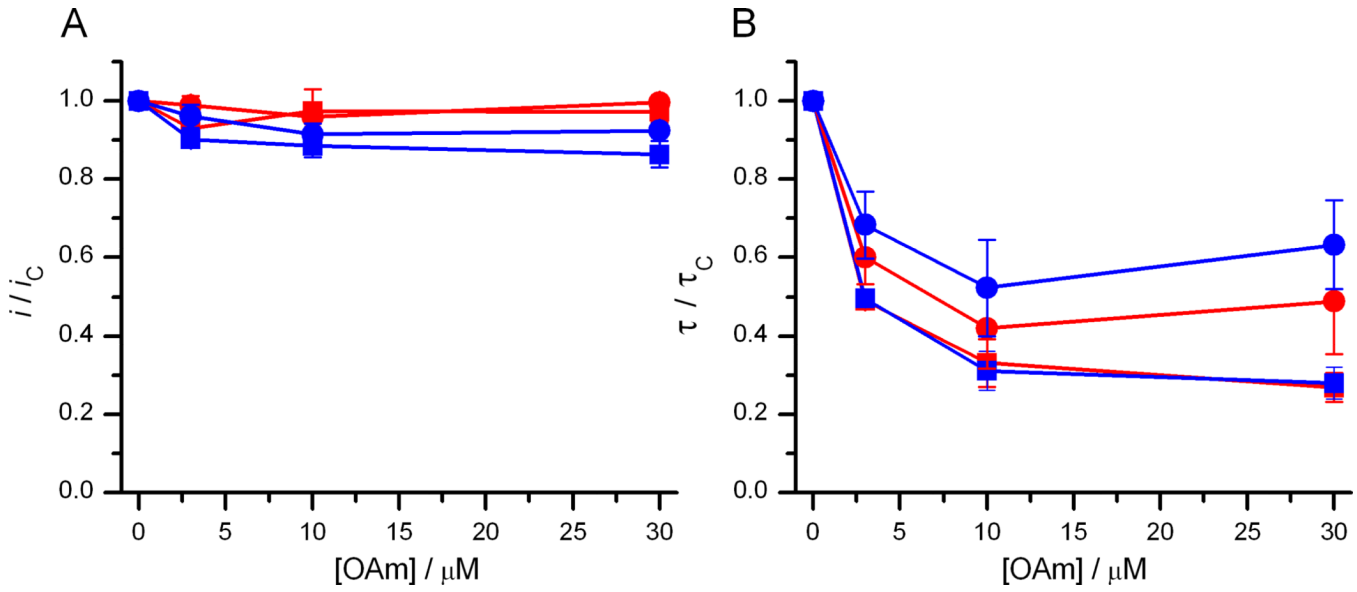

Figure 7.

Dose-response curves for OA at pH 7 and 9. Changes in *i* (**A**) and **τ**(**B**) for gA(13) channels (red) and AgA−(15) channels (blue) as functions of [OA]. Circles denote results at pH 7; squares denote results at pH 9. DOPC, 1 M NaCl, 10 mM HEPES (pH 7) or 10 mM Na_2HPO_4 (pH 9), 200 mV.

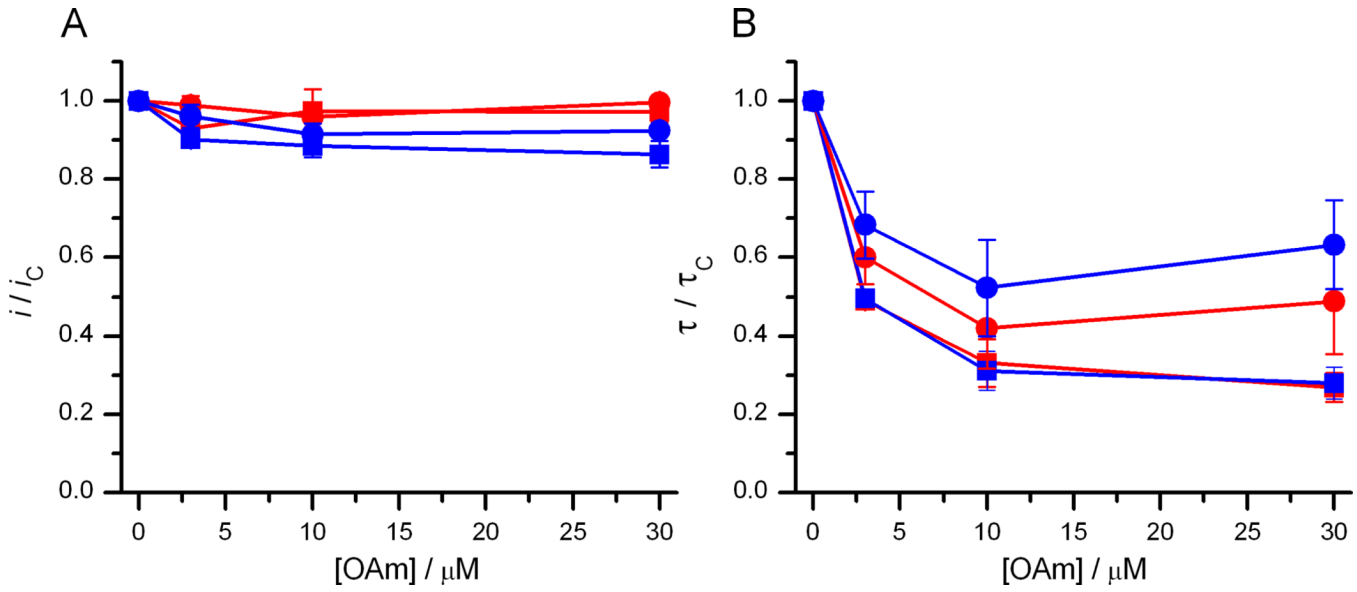

Figure 8.

Dose-response curves for OAm at pH 7 and 9. Changes in *i* (**A**) and **τ**(**B**) for gA(13) channels (red) and AgA−(15) channels (blue) as functions of [OAm] . Circles denote results at pH 7; squares denote results at pH 9. DOPC, 1 M NaCl, 10 mM HEPES (pH 7) or 10 mM Na_2HPO_4 (pH 9), 200 mV.

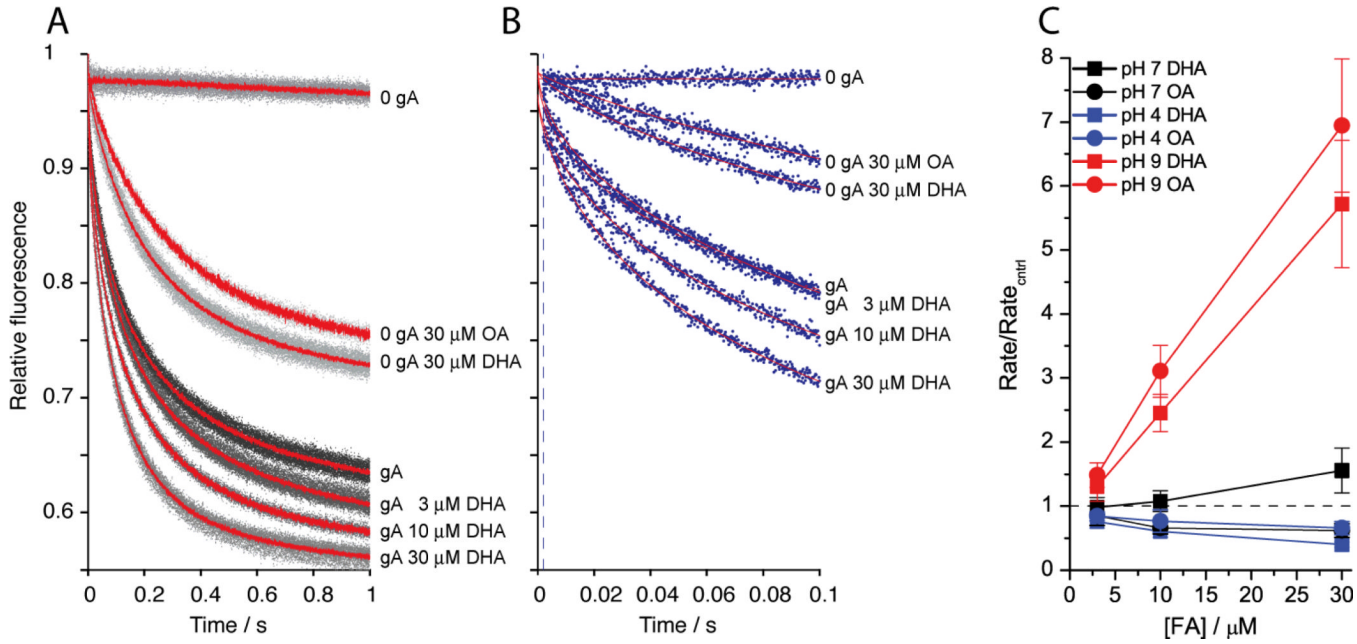

Figure 9.

DHA and OA alter gA channels function in hydrocarbon-free lipid vesicles. **A:** Effects of DHA and OA in the time course of the Tl^+-induced fluorescence quenching of ANTS encapsulated in LUVs (at pH 7). ANTS-containing $DC_{22:1}PC$ vesicles doped with gA were incubated for 10 min at 25 °C with increasing concentration of DHA (bottom four traces) or 30 µM OA (middle two traces) in the absence or presence of gA; the top trace was recorded in the absence of FA. Gray dots denote results from all repeats (n > 5 per experimental condition); red lines denote the average of all repeats for each condition. **B**: the first 100 ms from a single repeat for each condition; gray dots denote results, red lines are stretched exponential fits (2 – 100 ms) to these repeats. The stippled line denotes the 2 ms mark, the time at which the rate of quenching is determined. **C:** Normalized changes in fluorescence quench rates for DHA and OA at pH 4, 7 and 9 as functions of [DHA] or [OA]. The horizontal stippled line denotes no changes in the rate of quenching.

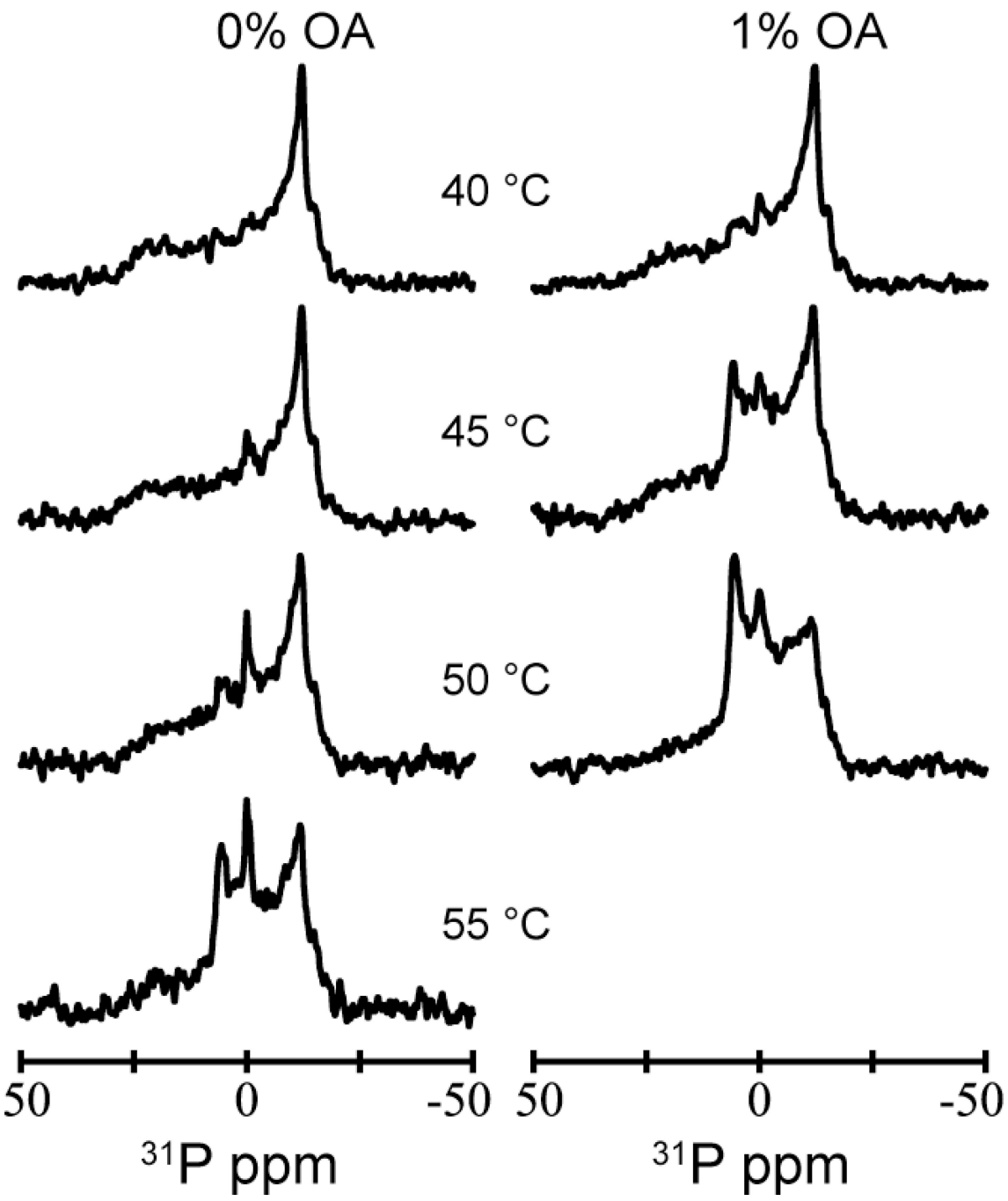

Figure 10.
Effect of OA on the lipid phase preference. ^{31}P NMR spectra of DOPC:DOPE (1:3) liposomes in the absence and presence of 1 mole percent OA at pH 7, measured at 40, 45, 50 and 55 °C (no OA) and 40, 45 and 50 °C (1 mole percent OA).

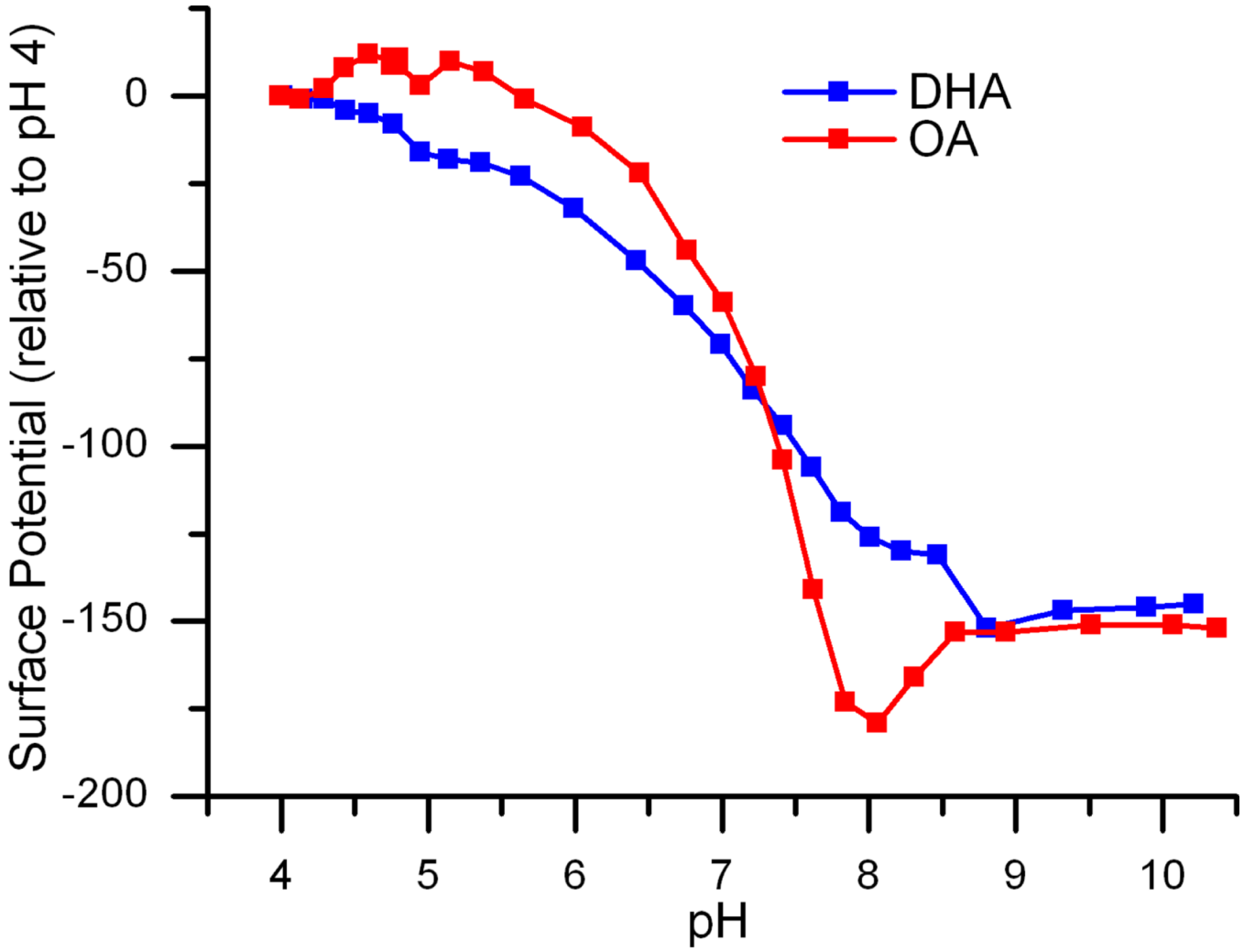

Figure 11.
Titration of fatty acids in DOPC monolayers. Changes in the surface potential of DOPC monolayers in the presence of 3 μM DHA or OA as functions of pH. The midpoint potential for each titration curve was determined from linear interpolation between the adjacent points.

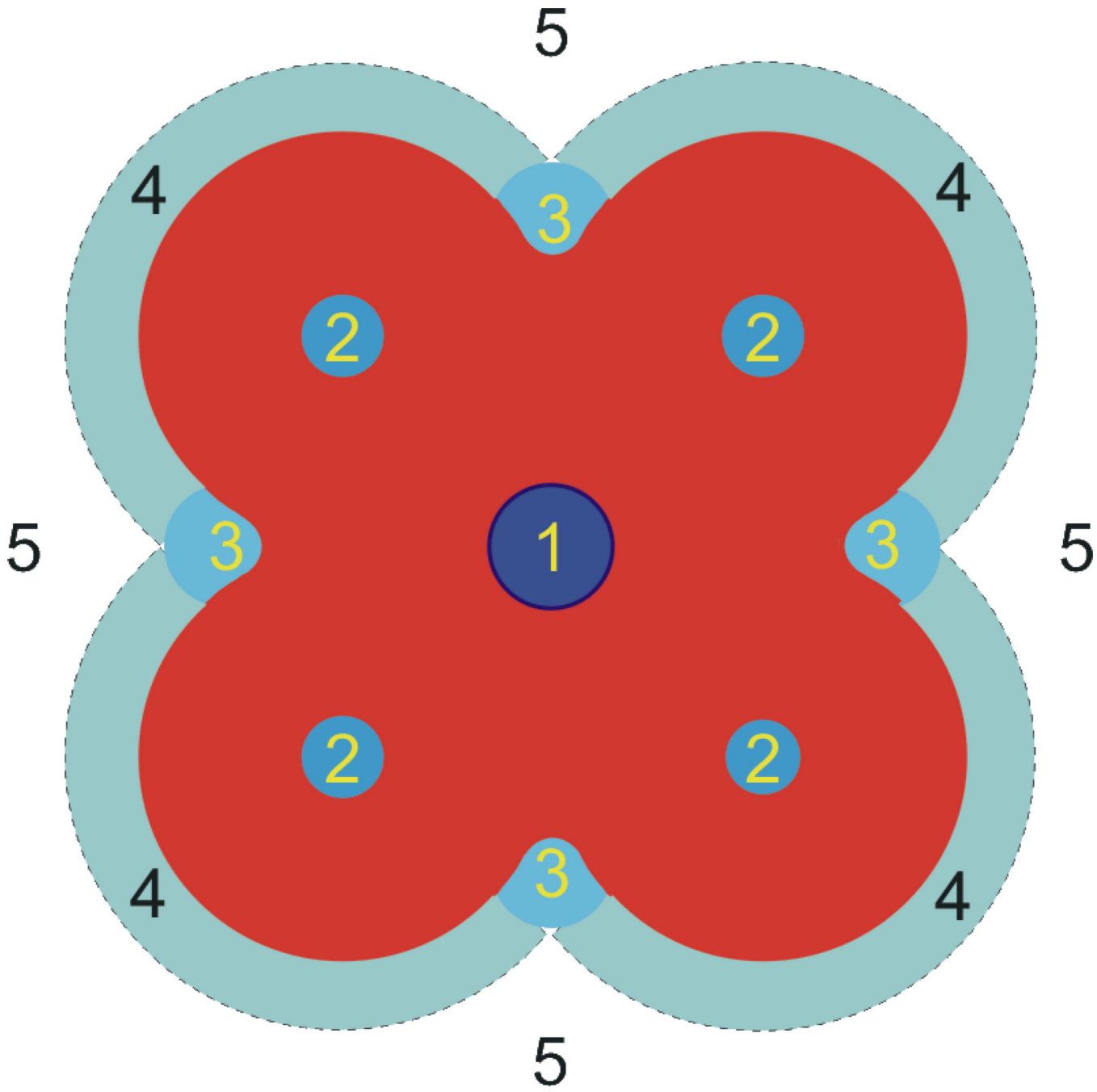

Figure 12.

Mechanisms by which drugs and other amphiphiles can inhibit membrane protein function: 1) occluding the pore or substrate binding site to block function; 2) binding to sites formed by the protein, to alter function by altering the free energy difference between different conformations $\Delta G^{\mathrm{I}\rightarrow\mathrm{II}}_{\mathrm{protein}}$, cf. Eq. 1; 3) binding to selective sites at the protein/bilayer interface, which may both $\Delta G^{\mathrm{I}\rightarrow\mathrm{II}}_{\mathrm{protein}}$+$\Delta G^{\mathrm{I}\rightarrow\mathrm{II}}_{\mathrm{bilayer}}$, cf. Eq. 1; 4) non-specific accumulation at the protein/bilayer interface to alter the local lipid packing and 5) partitioning at the bilayer/solution interface to alter lipid bilayer material properties, which both will alter $\Delta G^{\mathrm{M}\rightarrow\mathrm{D}}_{\mathrm{bilayer}}$, cf. Eq. 1 the bilayer contribution to the conformational equilibrium (Modified after [73]).

Table 1

Changes in gA channel lifetimes by changes in acyl chain unsaturation

	τ_{DOPC}	τ_{DHA}/τ_{DOPC}	$\tau_{DHA\text{-}ME}/\tau_{DOPC}$	τ_{PDPC}
gA(13) channels	17 ± 1 ms	2.2 ± 0.2	1.5 ± 0.2	49 ± 8 ms
AgA^{-}(15) channels	175 ± 7 ms	1.46 ± 0.08	1.17 ± 0.06	385 ± 30 ms
τ_{13}/τ_{15}	0.097 ± 0.003	1.5 ± 0.1	1.3 ± 0.10	0.13 ± 0.01

The subscripts denote lipid type or channel. τ_{13}/τ_{15} denotes the ratio of the relative changes in the lifetime of gA(13) channels relative to the changes observed for the AgA^{-}(15) channels

Table 2

Estimated transition temperature for the onset of the H_{II} phase

pH	0% Oleic Acid	1% Oleic Acid	~ ΔT
4	316 – 318 K	315–317 K	−1 K
7	322 – 324 K	312 – 314 K	−10 K

The transition temperature was estimated from linear interpolation of spectra similar to those in Figure 10.